FastRunner:
A Fast, Efficient and Robust Bipedal Robot.
Concept and Planar Simulation.

Sebastien Cotton, Ionut Mihai Constantin Olaru, Matthew Bellman,
Tim van der Ven, Johnny Godowski and Jerry Pratt

***Abstract*— Bipedal robots are currently either slow, energetically inefficient and/or require a lot of control to maintain their stability. This paper introduces the FastRunner, a bipedal robot based on a new leg architecture. Simulation results of a Planar FastRunner demonstrate that legged robots can run fast, be energy efficient and inherently stable. The simulated FastRunner has a cost of transport of 1.4 and requires only a local feedback of the hip position to reach 35.4 kph from stop in simulation.**

I. INTRODUCTION

Why is it that animals can run so quickly and gracefully while legged robots move slowly and unnaturally? One answer is that we still lack a complete understanding of how animals run fast. We also lack the engineering knowledge necessary to take what we learned from biological systems and apply it to mechanical systems effectively. Specifically, there are several technical issues that have made the design and control of fast running robots challenging. Most legged robots have direct linkages, transmissions with constant gear ratios, a lack of compliance and adverse motion dynamics. As a result, legged robots have typically been slow, inefficient and require computer control for stable locomotion. The purpose of the FastRunner project and this paper is to demonstrate that legged robots can run fast, be energy efficient, and be inherently stable.

The current record for the fastest legged robot is held by the Planar Biped of the MIT Leg Laboratory, which ran 21 kph in 1988 [1]. The Planar Biped was driven by a hydraulic actuator in series with a pneumatic spring. This kind of actuation outputs a great amount of power, but often requires an off-board power supply or the use of a gasoline engine, as is used on BigDog [2]. With such a large amount of available energy, robots utilizing this method of actuation are extremely capable and robust to disturbances, but they are not energy efficient. Electrically driven robots, such as Asimo, on the other hand, are typically more energy efficient, but no electrically driven robot has achieved significantly fast running yet.

Many great advances in energy efficiency have been made during the last few decades. Several studies dedicated to passive walkers, based on passive dynamics and limit cycle principles, have demonstrated that legged robots can walk without consuming energy and without control as long as they are walking down a slope without disturbances [3]. On flat ground, these passive walkers are limited to slow walking for a limited number of steps. Recently, the Cornell Ranger has extended the capacities of passive walkers through the addition of small electrical actuators, which provide just enough power to activate the robot's passive dynamics and propel it over long distances. However, with such minimal power and control authority, robots like the Cornell Ranger are relatively slow and lack significant recovery capabilities.

Previous research in the field of legged robots has shown that it is difficult to find a good balance between speed, energy efficiency and stability. However, nature has proven in numerous ways that this balance does exist, thus robots should be able to replicate, or at least approach, the capabilities of animals. With this philosophy in mind, we are developing the FastRunner, a high speed, efficient, dynamically stable bipedal robot. This robot utilizes a new leg architecture, which incorporates a network of elastic elements and concentrates its power input in a single main drive actuator. To date, the Planar FastRunner simulation has achieved running from 0 to 35.4 kph (= 22 mph = 9.8 $m.s^{-1}$) while being relatively energy efficient and inherently stable.

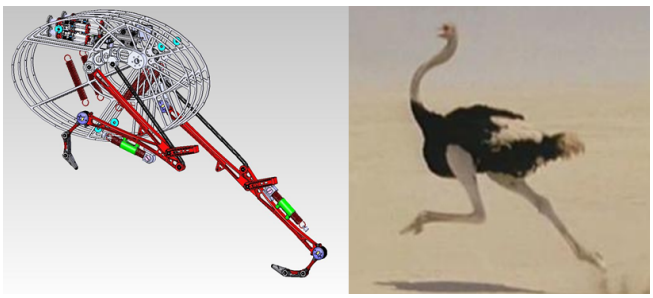

Fig. 1. Inspired by the ostrich (Struthiocamelus), the FastRunner robot has achieved stable running at 34.5 kph (22 mph) in simulation. Partial CAD model of the FastRunner on the left.

A video of the simulation results as well as the open source code of our simulation is available at http://www.ihmc.us/groups/fastrunner

This work is supported by The Defense Advanced Research Projects Agency (DARPA), under the Maximum Mobility and Manipulation (M3) program, BAA-10-65-M3-FP-024.

Authors are with the BioInspired Robotic Lab at the Institute for Human and Machine Cognition, Pensacola, Florida, 32502, USA.
{scotton,iolaru,mbellman}@ihmc.us
{tvanderven,jgodowski,jpratt}@ihmc.us

Even though much of the FastRunner architecture has been inspired by nature, several of the FastRunner design features have been previously identified by the biomechanics community. A fundamental observation made in the biomechanics literature is that fluctuations of the kinetic and gravitational potential energy during running occur in phase with each other [4], [5]. This observation leads to the conclusion that efficient running requires energy to be stored and released during each step. In the FastRunner leg architecture, energy storage is implemented using mechanical springs. Simple spring-mass models are capable of describing data gathered from human running experiments quite well [6], supporting the use of springs in our design. Several biomechanical studies have also shown that leg stiffness increases with speed [7], [8]. This key feature is achieved in the FastRunner design through non-linear profiles in some of the springs. The springs and their roles are presented in section II.

For legged animals, a specific set of muscles is active during each phase of the gait cycle [5]. This results in a hybrid system made of several dynamic modes where each mode is optimized for a specific duty. Previously, legged robots have not had such capabilities and, consequently, relied on a single dynamic mode to achieve their behavior. By implementing a mechanism to engage or disengage some of the springs according to the phase of the gait, the FastRunner benefits from having two dynamic modes, one which is optimized for the stance phase and another that is optimized for the swing phase. Implementation of this mechanism and the properties it enables are detailed in section II.

In terms of actuation, most of the bipedal robots with advanced capabilities are equipped with one actuator per degree of freedom, leading to high energy consumption. The FastRunner carries only one actuator per leg, located at the hip. The other motions, knee, ankle, toes, are actuated by a combination of passive linkages and passive dynamics, reducing the need for actuation at each of these joints and thereby reducing the energy consumption. The passive linkages emulate passive elements like tendons and ligaments and play a crucial role in the FastRunner architecture. The role of each passive linkage is described in section II.

Several studies have identified that smart mechanical design can lead to self-stabilizing properties, i.e. the ability to stabilize a system in the presence of disturbances without sensing the disturbance or its direct effects [9], [10]. With a similar philosophy, we successfully developed the FastRunner architecture so that the robot does not need global feedback control to run or to recover from small disturbances. This idea of mechanical intelligence calls for embedding the stability required for running directly into the leg architecture, leaving the control effort for special maneuvers. Simulation results demonstrating the capabilities of the FastRunner are presented in section III.

Based on the FastRunner simulation, we have started to build a functional robot. A preliminary prototype of the FastRunner leg is presented in section IV.

Finally, a general discussion and ongoing improvements to the FastRunner design are provided in the last section of this paper.

II. LEG ARCHITECTURE

The development of the FastRunner has been inspired by the fastest bipedal animal on earth, the ostrich, see Fig. 1. An average male ostrich is about 1.4 m tall at the hip and weighs around 100 kg. We scaled the FastRunner so that it has similar limb segment lengths and mass distributions. We conserved a height of 1.4 m at the hip, but we reduced the total mass of the robot to 30 kg. More information describing the biomechanical parameters of ostriches can be found in [11], [12], [13]. Instead of trying to replicate the full functionality of an ostrich's muscles, we identified the primary functions of each of the ostrich's major muscle groups that contribute to the essential aspects of running, in order to create a simplified yet functional planar model of the leg. This model ensures the same essential planar functionality without requiring the full multiplicity of elements. A schematic of the leg model is presented in Fig. 2.

A. Links and Joints

Six links and six joints constitute the main elements of the FastRunner robot. In Fig. 2, links are referenced with numbers, joints with lower case letters and springs with upper case letters. From the top to the bottom, the links are: the femur (1), the tibia (2), the foot (3), and three toe segments:

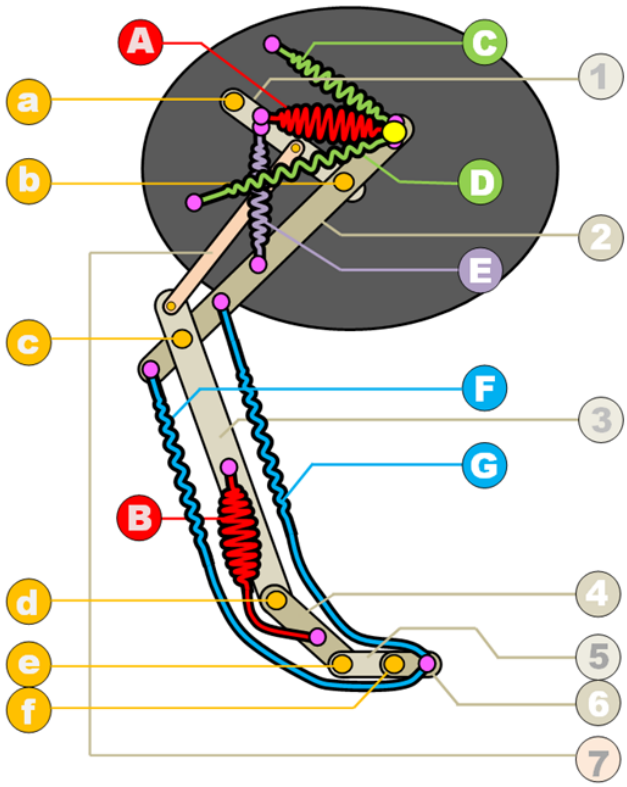

Fig. 2. FastRunner Schematic: Joints, Springs and Links.

the first toe segment (4), the second toe segment (5), and the third toe segment (6). The six pivot joints are: the hip (a), the knee (b), the ankle (c), the first toe joint (d), the second toe joint (e), and the third toe joint (f). Along with the tibia, a seventh link called the Achilles linkage (7) creates a closed-loop four bar mechanism, coupling the knee to the ankle with a 1:1.5 transmission ratio. This linkage allows us to reduce the required number of actuators and acts as a foot velocity amplifier. Contrarily to classical legged robots that use point feet or flat feet, the FastRunner utilizes a foot architecture made of three toe segments. As indicated in [14], toes are important in running because they allow the feet to roll as they push off at the end of the stance phase, resulting in a smoother trajectory of the center of mass. This rolling motion also eliminates the need for active ankle torque to move the center of mass in front of the stance foot, an approach often used in conventional legged robots.

B. Suspensions

Two suspension elements are used in the FastRunner leg to store and release the energy caused by gravity forces during running. They are represented in red and referenced with upper case letters on the FastRunner schematic, Fig. 2. A first suspension called *knee suspension* (A), is attached from the femur (1) above the hip (a) to the tibia (2) above the knee (b). Some of the energy stored in this suspension is kinematically converted into forward thrust during the energy release phase thanks to the leg architecture. This suspension is implemented with a non-linear spring active only during stance. By doing so, the leg inhabits two different dynamic modes. In the first mode, the knee suspension is active during stance, supporting the body weight. In the second mode, the knee suspension is inactive during swing, allowing for a full radial contraction of the leg which increases the ground clearance. With the leg retracted, the leg moment of inertia is reduced as the leg pulls in, reducing the amount of energy required to swing the leg forward. A second suspension called *toe suspension* (B), providing mainly upward thrust and counteracting the effect of gravity, is attached from the foot (3) to the first toe segment (4), crossing the first toe joint (d). This suspension is implemented with a spring in series with a cable, crossing the first toe joint with the help of a pulley. This kind of configuration based on springs, cables and pulleys emulates a muscle connected to bones through tendons and will be referenced in the rest of the paper as *tendon networks*. The toe suspension (B) starts applying a torque around the first toe joint (d) when the first toe segment (4) flexes forward. This torque is used to push off with the toes. When the toes are curled backward the toe suspension is slack, providing no torque around the first toe joint (d).

C. Swing elements

Three non-linear springs are used to enhance the swing motion of the leg (in green or purple on Fig. 2). A set of two non-linear springs are used to extend the leg at the end of swing. The *front extensor spring* (C) and *back extensor spring* (D) are respectively used to extend the leg at the end of the backward and forward swing. Leg extension is necessary at the end of the forward swing to prepare the leg for landing. The front extensor spring (C) is attached from the body (0) below and behind the hip (a) to the tibia (2) above the knee (b). The back extensor spring is attached from the body (0) above and in front of the hip (a) to the tibia (2) above the knee (b). A third spring called *passive swing spring* (E) is attached from the femur (1) above the knee (b) to the tibia (2) below the knee (b). This spring retracts the leg during swing.

D. Toe flexion and extension

One of the biggest challenges to get the robot running in simulation was to passively actuate its toes. The toes must flex (curl down/backward) when the leg is swinging forward to increase the ground clearance and they must extend at the end of the forward swing phase to prepare for ground contact. To achieve these desired effects, two tendon networks are used (in blue on Fig. 2). One, called *toe extension tendon network*, is attached from the tibia (2) above the ankle (c) to the third toe segment (6), crossing the three toe joints (d), (e) and (f). When the leg extends, the spring (G) is stretched and pulls on the cable connected to the third toe segment, causing the toes to extend. The other tendon network, called *toe flexion tendon network*, is attached from the tibia (2) below the ankle (c) to the third toe segment (6), crossing the three toe joints (d),(e) and (f). When the leg is retracted, the spring (F) is stretched and pulls on the cable connected to the third toe segment, causing the toes to flex (curl down/backward).

E. Actuation

Only one actuator per leg is currently used to generate the gait pattern of the FastRunner. This force-controlled actuator creates a torque around the hip joint axis. All of the other joints are actuated passively. The knee joint is actuated by the inertia of the lower links during swing and by the ground reaction forces and knee suspension during stance. The ankle and toe joints are coupled to the knee joint through the Achilles linkage and the tendon networks. For convenience, the actuator is not represented on Fig. 2.

F. Mechanical Parameters

Table I summarizes the length, mass and center of mass of the FastRunner main links. Center of mass of each link is given from its parent joint. Lengths and center of mass positions are in millimeters, masses are in kilograms.

TABLE I
MECHANICAL PARAMETERS OF THE FASTRUNNER LEG

Link	Length	Mass	CoM
Femur	283	2.1	153
Tibia	637	1.5	242
Achilles	654	0.3	327
Foot	531	1.5	260
Toe1	142	0.6	71
Toe2	106	0.45	53
Toe3	71	0.3	35

Each leg has a total mass of 6.75 Kg and a total length of 1.77 m. Body dimensions are 1.05 m x 0.65 m x 0.65 m and weighs 55% of the robot total mass (30 Kg). Table II summarizes the range of motion of each joint.

TABLE II
RANGE OF MOTION OF THE FASTRUNNER JOINTS

Joint	θ_{min}	θ_{max}
Hip	-90	10
Knee	50	115
Ankle	-155	0
Toe1	-90	60
Toe2	-50	60
Toe3	-30	30

Some of the elements referenced previously are based on non-linear springs. Non-linearity is essential in the profile of these springs to ensure their functionalities over a large range of speed. Non-linear profiles are implemented by several means, either by using a non-linear stiffness or by using a non-linear elongation. In our design, non-linear stiffness profiles are achieved by using two or more springs in series with different spring rates. Non-linear elongation can be achieved by using a linear spring connected to two links joined with rotary joints. As such, when the joint angles change the spring elongation follows a non-linear profile. These two techniques can also be combined to create more complex non-linear profiles. Force profile of such arrangement are

$$\begin{aligned} F &= kx + b\dot{x} \\ \text{with: } k &= k_i \text{ for } x_{i-1} < x \leq x_i \text{ and } x = f(q) \end{aligned} \tag{1}$$

where F is the total force exerted by the non-linear spring, k is the spring constant, x is the spring elongation, b is the spring damping, $\dot{x}$ is the spring velocity and $f(q)$ is a function of the joint angles q. Spring profiles have been tuned in simulation such that the robot is able to support its own body weight when static, and such that the legs exhibit a succession of contraction and extension when the legs swing back and forth.

III. SIMULATION RESULTS

A. Simulation environment

Based on the leg architecture presented in section II, we implemented a model of the FastRunner robot in the *Yobotics Simulation Construction Set* simulation environment. This environment has been successfully used in the past to design and control several robots such as Spring Flamingo and M2V2 [15], [16]. It allows for using similar algorithms to control simulated robots and their real versions with only slight changes, which illustrates quite realistic simulation properties. The simulation uses a Runge-Kutta 4^{th} order integrator with a step size of $10^{-5}s$. Ground contact is modeled through rigid spring-dampers (penalty method). We developed specific toolboxes for the FastRunner robot in order to implement and tune easily the profiles and attachment points of the various springs and tendon networks. Fig. 5 shows the Planar FastRunner simulation. A video is provided

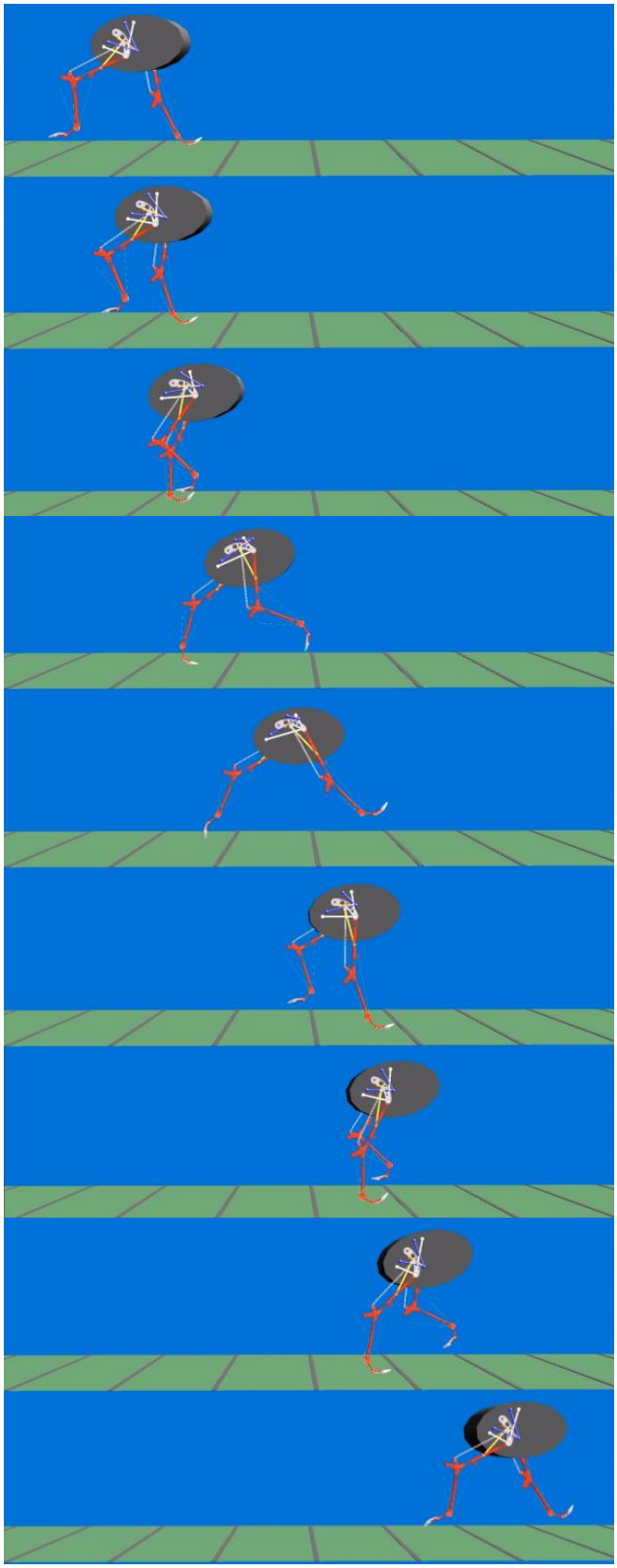

Fig. 3. Snapshots of the simulated FastRunner running at 35.4 kph. Ground lines are spaced by 1 m. Time between the first and the last snapshot is approximately 0.4s. At 35.4 kph, the FastRunner has a duty factor of 30%.

along with this paper to show the simulation results. Source code and instructions for running the simulation are available at http://www.ihmc.us/fastrunner.

B. Control

One of the main ideas behind the FastRunner concept was to embed self-stabilizing properties directly into the robot architecture. The FastRunner architecture presented in section II has sufficient mechanical intelligence to allow the robot to run with only local joint control at the hip. Stabilization does not require feedback of any global information, such as body velocity or body orientation, which are typically controlled through active feedback on most powered legged robots. While the current simulation only uses local hip joint feedback, we intend to use global state-based control feedback for special maneuvers and enhanced robustness over rough terrain. Example of special maneuvers include recovering from large disturbances or stepping in a specific location if required. As such the control architecture can be seen as a two stage controller. In this paper, only the first stage of the controller is used, which means that no global state-based feedback has been used, only the mechanical intelligence embedded in the leg is used to absorb small disturbances. These disturbances are mechanically absorbed by the leg due to its compliance. Consequently, we achieved running in simulation by only tracking a desired sinusoidal trajectory at the hip, calculated according to

$$\theta_{hip} = A \sin(2\pi f + \phi + \psi) + \theta_0 \quad (2)$$

where A is the hip motion amplitude, f is hip the oscillation frequency, ϕ is the phase difference between the left and right leg (For example, $\phi = 0$ for the left hip and $\phi = \pi$ for the right hip), ψ is the phase offset required to avoid discontinuities when the frequency f changes and θ_0 is the amplitude offset.

This trajectory is followed by the actuator thanks to a high gain proportional controller (with $K_p = 100000N/rad$). To increase the velocity of the robot, we modulated the sinusoidal trajectory amplitude and frequency over time. The changing rate of frequency and amplitude has a direct effect on the robot acceleration and speed. Small changing rates are preferred to avoid the introduction of large disturbances. Fig. 4 is an example of the trajectory at the hips used to get the robot running. Before applying this trajectory to the FastRunner's hip, the robot leans forward by swinging one of its legs for a half second, generating a small initial forward velocity. The right and left hip trajectory have a phase difference of π.

C. Running fast

We successfully reached 35.4 kph from stop in simulation. We are confident that the FastRunner architecture is capable of reaching higher speeds with better tuning of the mechanical parameters. During our simulations, the FastRunner architecture has proven stable running capabilities over a large range of speeds and not only at its top speed. To run at its top speed, the sinusoidal trajectory of the hip had a frequency of 2 Hz, which is a relatively low frequency in comparison with the top speed reached, 35.4 kph. Several architectural elements contribute to the FastRunner's high speed running capabilities. First, the Achilles linkage (7) acts as an angular velocity amplifier between the knee and the ankle joints. Second, the length of the leg is not fixed. Instead, it varies between a minimal length occurring during the full retraction at mid-swing to a maximal length occurring at the full extension of the leg at the end of the swing phase, increasing the leg end point velocity. The cyclic motion created by a succession of retraction and extension is the result of the combined effects of the leg inertia and the elastic elements (springs and tendon networks). Non-linear profiles of the elastic elements are tuned to take advantage of the natural leg's inertia, not to fight it, over the whole range of achieved speeds (from 0 to 35.4 kph in our simulations). As such, adverse dynamics motion are reduced while passive dynamics motion are enhanced.

Fig. 5 shows the velocity of the Planar FastRunner simulation over time. The FastRunner accelerated at 1.85 $m.s^{-2}$ and reached its top speed in about 7s. This figure also shows that the vertical oscillation of the center of mass are decreasing when the velocity of the robot increases. While running, the FastRunner has a large flight phase with a duty factor of 30%. The duty factor correponds to the percentage of the running cycle where the robot is on the ground. This flight phase is illustrated in Fig. 3. At full speed, the ground contact duration is about 200ms. As shown in Fig. 6, the simulated FastRunner is significantly faster than other legged robots. We are currently working on developing the real FastRunner robot to verify that these speeds can be achieved.

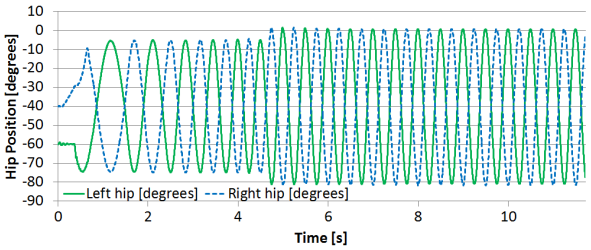

Fig. 4. Example of hip trajectories used to get the simulated FastRunner running without state-based control feedback.

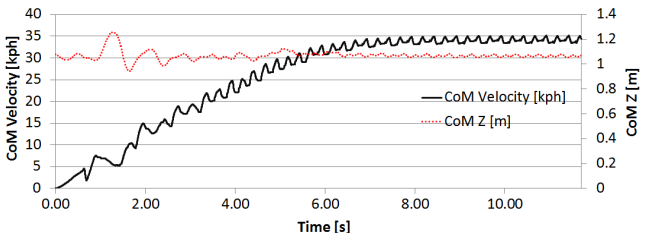

Fig. 5. Velocity and vertical position of the center of mass of the simulated FastRunner from 0 to 35 kph.

D. Energy efficiency

With the exception of passive walkers, most of the actuated legged robots lose significant energy during walking or running. The FastRunner architecture stores energy in various springs and releases it when necessary. As such, only a fraction of the energy required to propel the FastRunner needs to be produced by the actuators. By passively actuating five of the six main joints of the FastRunner, we largely reduced the need for active actuation and, consequently, energy consumption. Two reasons motivate the choice of passive actuation. First, passive walkers have proven that a legged structure can walk with minimal energy consumption by using its own inertia. Second, the biomechanical literature shows that dynamic coupling exists between several joint motions of a leg [5]. By analyzing the joint motions of an ostrich, we identified those joint couplings and reproduced them with passive actuation. Standing is usually a task requiring energy consumption, since it takes energy to maintain the rest position of each joint of the legs. FastRunner avoids this issue by taking advantage of its passive elements. Each spring is tuned to provide the exact amount of force necessary to counteract the gravity effect in the rest position. With a center of mass ground projection located exactly in the middle of the base of support, the FastRunner remains static in its rest position and no energy is consumed. With all of these elements reducing the energy required for running, the simulated FastRunner has a relatively low cost of transport. A comparison of the cost of transport versus maximal speed of several robotic platforms, including the simulated FastRunner, is provided in Fig. 6. The cost of transport is a unitless index allowing to measure the efficiency of a system and is calculated with $CoT = energy/(weight * distance)$. While running at its top speed, 35.4 kph, the simulated FastRunner has a cost of transport about 1.4.

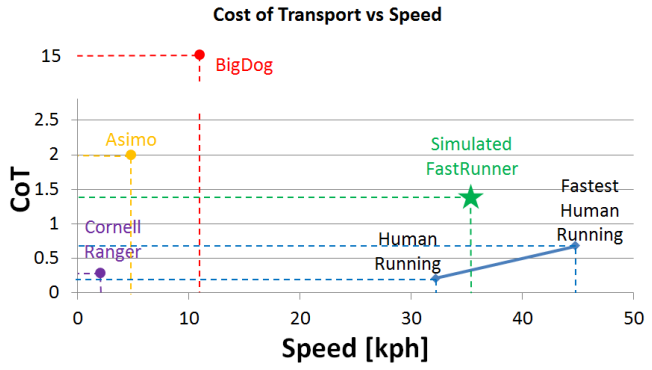

Fig. 6. Cost of transport and top speed comparison between the simulated FastRunner and other robots.

This number has been calculated by measuring directly the absolute value of the power input at the hip. This cost of transport should slightly increase when we include motor inefficiencies, power supply efficiency, etc. However, we are confident that we can further reduce the cost of transport through optimizing the leg parameters and driving function. We are hopeful that FastRunner architecture will achieve similar speeds and energy efficiency as observed in nature.

E. Robustness

We tested the FastRunner architecture's robustness to disturbances without feedback from the global state-based controller to evaluates its recovery capabilities. Two tests were conducted with the robot running at its full speed. We first tested the FastRunner's ability to recover from a step down. FastRunner was able to recover for a step down up to 7.5 cm height, which represents 5% of the hip height. The second test consisted of running over up and down slopes. FastRunner was able to successfully climb or go down slopes up to a 10% incline. Both results emphasize that mechanical intelligence embedded in the leg architecture reduces the need for control. Fig.7 shows the simulation running from 0 kph to 35.4 kph and reaching stable steady state at different speeds in this range.

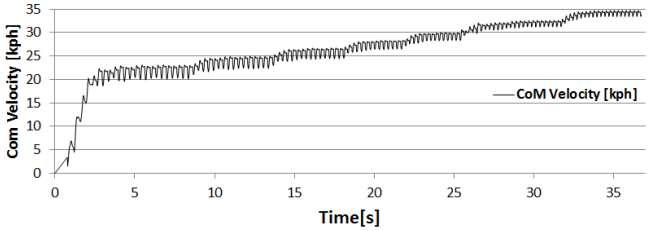

Fig. 7. The simulated FastRunner demonstrates stable steady state capacities over a large range of speed.

IV. HARDWARE

The FastRunner robot has been partially modeled in a CAD environment, see Fig. 1. In Fig. 8, a mockup of the leg, based on the simulation model of the FastRunner, has been assembled to demonstrate the behavior of the leg and to analyze potential risks. This mockup reproduces faithfully the length of each link, position and range of motion of each joint. Tendon networks have been implemented and have demonstrated passive toe actuation as expected. During the design process we identified three main components that need further investigations. First, the knee suspension engagement mechanism must be able to engage the knee suspension spring in less than 20 ms for any configuration of the leg and hold forces up to 3500 N. Second, recreating exact non-linear profiles as they are in the simulation model may be challenging. Several iterations between the simulation and the real design have been necessary in order to choose mechanically feasible non-linear springs. Finally, slack removal mechanisms are still under investigation to compensate for the change in length of the tendon network cables. Actuation will be achieved through Series Elastic Actuators [17]. The benefits of using series elastic actuation include back drivability, low impedance, low friction and good force control bandwidth.

V. DISCUSSION AND FUTURE WORK

FastRunner's novel architecture has demonstrated in simulation fast, efficient, stable bipedal running at speeds approaching human performance. The mechanical design for a physical robot prototype capable of emulating these speeds and performance metrics is currently in progress. This design, replicating the simulation model, appears reasonably feasible with available technology. We believe that by optimizing the mechanical parameters and driving function, we will be able to reduce the loads in the elements, improve the energy efficiency and increase the speed of FastRunner. FastRunner has also demonstrated that robustness and stable running can be more easily managed when a sufficient level of mechanical intelligence is embedded into the robot architecture, reducing the need for complex control algorithms. Robustness to small disturbances while running at high speed has also been demonstrated and we are hopeful to demonstrate running over rough terrain at moderate speeds. We believe that some of the concepts presented in this paper have some stabilization effects. First, having the center of mass located below and in front of the hip seems to play an important role on the FastRunner's stabilization. Second, we observed that adding non-linearity to some of the elastic elements allowed the FastRunner for reaching higher speed, suggesting that non-linearity is relevant to robustness while running at different speeds. More specifically, FastRunner has demonstrated stable steady state over its whole range of speed. By analyzing the FastRunner's energy expenditure versus running speed curve, we observed that the FastRunner has a preferred running speed, similarly to legged animals. More specifically, we have been able to change the efficiency point on this curve by tuning the elastic elements and hip trajectory. Based on these considerations we assume that the FastRunner architecture can be optimized for some objective functions, such as energy efficiency for given speeds. We will try to verify these hypotheses in our future developments. We also plan to utilize a global state-based controller to achieve special maneuvers. Several design elements are still under investigation and, we hope, will help in reducing the gap between robots and nature.

Fig. 8. Prototype of the FastRunner leg showing main links and joints.

REFERENCES

[1] J. Koechling and M. Raibert, "How fast can a legged robot run?" in *ASME Symposium on Dynamic systems and Controls Division*, 198.

[2] R. Playter, M. Buehler, and M. Raibert, "Bigdog," in *SPIE Unmaned Systems Technology VIII*, 2006.

[3] T. McGeer, "Passive dynamic walking," *International Journal of Robotics Research*, vol. 9, pp. 62–82, 1990.

[4] R. Margaria, P. Cerretelli, P. Aghemo, and G. Sassi, "Energy cost of running," *Journal of Applied Physiology*, vol. 18, pp. 367–370, 1963.

[5] J. Rose and J. G. Gamble, *Human Walking, Third Edition*, J. Rose and J. G. Gamble, Eds. Williams and Wilkins, 2005.

[6] H. Geyer, A. Seyfarth, and R. Blickhan, "Compliant leg behavior explains basic dynamics of walking," *Philosophical Transactions of the Royal Society,*, vol. 273, pp. 2861–2867, 2006.

[7] T. McMahon and G. C. Cheng, "The mechanics of running: How does stiffness couple with speed?" *Journal of Biomechanis*, vol. 23, pp. 65–78, 1990.

[8] S. Kim and S. Park, "Leg stiffness increases with speed to modulate gait frequency and propulsion energy." *Journal of Biomechanics*, vol. 44(7), pp. 1253–1258, 2011.

[9] H. Geyer, A. Seyfarth, and R. Blickhan, "Natural dynamics of spring-like running: Emergence of selfstability." in *Proceedings of the International Conference on Climbing and Walking Robots*, 2002.

[10] R. Blickhan, A. Seyfarth, H. Geyer, S. Grimmer, H. Wagner, and M. Gunther, "Intelligence by mechanics," *Philosophical Transactions of the Royal Society*, vol. 365(1850), pp. 199–220, 2007.

[11] S. M. Gatesy and A. Biewener, "Bipedal locomotion: effects of speed, size and limb posture in birds and humans," *Journal of Zoology*, vol. 224, pp. 127–147, 1991.

[12] J. Rubenson, D. G. Lloyd, T. F. Besier, D. B. Heliams, and P. Fournier, "Running in ostriches (struthio camelus): three-dimensional joint axes alignment and joint kinematics," *Journal of Experimental Biology*, vol. 210, pp. 2548–2562, 2007.

[13] S. M. Gatesy, M. Baker, and J. Hutchinson, "Constraint-based exclusion of limb poses for reconstructing theropod dinosaur locomotion," *Journal of Vertebrate Paleontology*, vol. 29(2), pp. 535–544, 2009.

[14] P. Adamczyk, S. Collins, and A. Kuo, "The advantages of a rolling foot in human walking," *Journal of Experimental Biology*, vol. 209, pp. 3953–3963, 2006.

[15] J. Pratt and B. Krupp, "Design of a bipedal walking robot," in *Proceedings of the SPIE*, 2008.

[16] J. Pratt, "Exploiting inherent robustness and natural dynamics in the control of bipedal walking robots," Ph.D. dissertation, Massachusetts Institute of Technology, Cambridge, Massachusetts, 2000.

[17] G. Pratt, M. Williamson, P. Dillworth, J. Pratt, K. Ulland, and A. Wright, "Stiffness isn't everything," in *International Symposium on Experimental Robotics*, 1995.